An evaluation of radial track etch rate in LR-115 detectors exposed to Fe ions by means of FT-IR spectrometry

Yamauchi, Tomoya
Watanabe, Souichiro
Oda, Keiji
Yasuda, Nakahiro
Barillon, Remi

(Citation)
Radiation Measurements,43(Supplement 1):S116-S119

(Issue Date)
2008-08

(Resource Type)
journal article

(Version)
Accepted Manuscript

(URL)
https://hdl.handle.net/20.500.14094/90000770

MS826p

An evaluation of radial track etch rate in LR-115 detectors exposed to Fe ions by means of FT-IR spectrometry

T. Yamauchi[a*], S. Watanabe[a], K. Oda[a], N. Yasuda[b], R. Barillon[c]

[a] Kobe University, Graduate School of Maritime Sciences, 5-1-1 Fukaeminami-machi, Higashinada-ku, Kobe 658-0022, Japan

[b] National Institute of Radiological Sciences, 4-9-1 Anagawa, Chiba 263-8555, Japan

[c] Institut Plurisdisciplinaire Hubert Curien (UMR 7178), 67037 Strasbourg Cedex 2, France

Chemical modification of LR-115 induced by the irradiation of gamma-ray and 147 MeV Fe ions has been observed. Density of $O-NO_2$ and C-O-C bonds in the sheets was decreased. We also confirmed the modification by chemical etching during early stage in LR-115 exposed to Fe ions. The absorption band around 1740 cm^{-1} was reduced rapidly, which can be attributable to C=O bonds of some additives contained in LR-115. We have derived the radial track etch rate from the reduction of the absorbance.

PACS: 61.80.Ed; 61.62.Pv

Keywords: Radial track etch rate; Latent track; Track chemistry; LR-115; FT-IR

*Corresponding author: Tomoya Yamauchi

Phone: +81-78-431-6307

Fax: +81-78-431-6369

e-mail: yamauchi@maritime.kobe-u.ac.jp (Tomoya Yamauchi)

1. Introduction

Under an optical microscopic-scale, the two-velocity-model describes well the evolution of etch pit by chemical etching. We must take into account, however, the radial size of latent tracks under nano or submicron-scale (Fromm, 2005). To assess the radial track etch rate, conductmetric technique has been widely applied for various kinds of polymers exposed to heavy ions (Apel et al., 2006), as well as a method of folding track replica (Bernaola et al., 2006). It was insisted that the conductmetric method contained some questions to be solved (Enge, 1995). Recently, the role of the produced small molecules on the formation of the track halo was examined by low temperature irradiations (Apel et al., 2006). The influence of UV light on the latent tracks was also investigated (Zhu et al., 2005). The assumption of conical track shape was examined in the first conductmetric study for CR-39 (Oganesyan et al., 2005). On the other hand, some spectral studies have been made to study the chemical etching process of ion-irradiated polymers (Zhu et al., 2006). It was found that the track etching could be monitored by FT-IR method for thin film materials (Sertova et al., 2005).

In this work we have observed chemical modification of LR-115 induced by the irradiation of gamma-ray and 147 MeV Fe ions. The modification during the early stage of chemical etching was also examined by FT-IR method. We have derived the radial track etch rate from the reduction of the typical absorption band on the assumption that the etched track was cylindrical.

2. Experiments

LR-115 sheets, supplied from DOSIRAD, France, consist of a mixture of cellulose dinitrate and cellulose trinitrate with a density of 1.4 g/cm^3 (Doerschel et al., 2003). About 10 % of the weights are some additives (Barillon et al., 2003).

Gamma-irradiation was made at an intense Co-60 source in the Institute for Scientific and Industrial Research, Osaka University, Japan. During the exposure, the films were sandwiched by PMMA sheets with 2 mm thick to achieve the electron equilibrium condition. The absorbed doses were 100, 200 and 300 kGy and the dose rate was 1.2 Gy/s. Fe ion exposure was performed in air at the medium energy irradiation system of Heavy Ion Medical Accelerator in Chiba (HIMAC), NIRS, Japan (Yasuda et al., 2005). The incident energy of Fe ions on the films was 147 MeV. The fluences were 5.7x10^9, 1.2x10^{10} and 2.3x10^{10} ions/cm^2.

FT-IR measurements were performed for each film both before and after the irradiation, using FTIR-8400S (SHIMADZU, Japan). The bulk etch rate of LR-115 in a stirred 2.5 N NaOH solution at 50 ˚C was determined to be 0.28 nm/s by the fission fragment method. This is concordant with recent other works (Barillon et al., 1997; Marocco et al., 2001; Doerschel et al., 2003; Yip et al., 2006). Short-time etching described in the following section was also made in this condition.

3. Results and discussions

3.1. Effects of exposure to gamma-ray and Fe ion

The band assignments of LR-115 for major ones were given in the literatures (Kovalenko et al., 1992; Barillon et al., 1999). In the followings, we pay our special attention to the bands at 1146 cm^{-1} (glycosidic bonds), 1600 cm^{-1} (nitrate function) and 1740 cm^{-1} (carbonyl bonds).

Figure 1 shows FT-IR spectra of LR-115 films with and without the gamma-irradiation, indicating the significant decrease of the absorbance at the glycosidic bonds and nitrate function (Barillon et al., 1999&2003). The relative absorbance, A/A_0, was attained for each fluence, where A_0 is the original net absorbance of the considering bonds. The A/A_0–value is equal to the survival fraction, N/N_0, which is the ratio of the number density of the considering bond, N, to the original one, N_0. The results are presented in Fig. 2, showing that A/A_0 decreases linearly with the absorbed dose for both bonds. Therefore, we obtained the following simple experimental formula,

$$N / N_0 = 1 - k_i \cdot D, \qquad (1)$$

where D is the dose in Gy and k_i is a constant for the bond i (in Gy^{-1}). The constant k_i enable us to evaluate G-values for the scissions of glycosidic and nitrate bonds par 100 eV, utilizing the following relation:

$$G = 9.64 \times 10^6 N_0 k_i, \qquad (2)$$

where N_0 is in mol/kg. The calculations led G-values of 58 and 74, respectively for glycosidic and nitrate bonds (see Table 1). Barillon had emphasized the role of the additives contained in LR-115 and noted the extended chemical reaction, in understanding these lager G-values (Barillon, 2005).

Figure 3 indicates the changes in the relative absorbance by Fe ion irradiation as a function of the fluence. It decreases linearly with the fluence. Then we are able to give the experimental formula as,

$$N / N_0 = 1 - \sigma_i \cdot F, \tag{3}$$

where F is the fluence in ions/cm^2 and σ_i is a constant for the bond i in cm^2. The latter was the effective track area where the bonds in question were lost, from which we can derive the track core radius as given in Table 1. It also enables us to calculate the G-values, using the fundamental relation as,

$$G = 8.43 \times 10^{15} \frac{\sigma_i N_0}{LET}, \tag{4}$$

where LET is in keV/μm. In this case, the mean LET of Fe ion in the films were 5200 keV/μm. We could not find the significant LET dependence here (see Table 1).

3.2. Radial track etch rate

Short-time etchings with 1 second and FT-IR measurements were repeated for Fe ion irradiated sheets. The absorption band around 1740 cm^{-1} was reduced rapidly, which can be attributable to C=O bonds in additives, while the density of other bonds hardly changed, as shown in Fig. 4. Changes in the relative absorbance with etching time are shown in Fig. 5 for three different fluences, where lines represent their simple fits. When the etch pits are cylindrical and not overlapped each other, we can apply the following formula as,

$$A / A_1 = 1 - \pi r_e^2 \cdot F, \tag{5}$$

where r_e is the pit radius and A_1 is the net absorbance before etching. Namely,

$$r_e = \sqrt{\frac{1}{\pi F}\left(1 - \frac{A}{A_1}\right)}. \tag{6}$$

Data points and the fitted lines in Fig. 5 were converted into the radius using eq. (6), then we obtained the effective etch pit radius against the etching time, as shown in Fig. 6. Contrary to our expectation, we could not diminish the fluence-dependence by this conversion. This could be partly caused by the track overlapping. And data of the lowest fluence at short etching times are hard to treat. The slope of the growth curves is the radial track etch rate at the etching time or the etch pit radius. In the early stage, therefore, the radial track etch rate is significantly higher than that of bulk etching (showing by broken line in Fig. 6). By the way of trial, we obtained the radial track etch rate by differentiating the growth curve of the medium fluence with respect to the etching time, and expressed it as a function of the radial distance, as shown in Fig. 7.

Although we did not obtained the experimental value more than 18 nm as radial distance, the curve and bulk etching show that the area with enhanced track etch rate was within 36 nm. It might be possible to regard this as a track core radius. The radiation sensitive parts glycosidic and nitrate bonds, were selectively lost in the track core by the irradiation, and the subsequent etching will remove rapidly remained segments of additives in that region.

4. Closing remarks

As a preliminary study, the radial track etch rate of Fe ion track in LR-115 was assessed through FT-IR spectrometry. We are now making additional experiments using other types of heavy ions and for different film materials.

Acknowledgements

The authors express heartfelt thanks to Mr. T. Ikeda, Dr. Y. Honda and Prof. S. Tagawa on the help of gamma-irradiation. The authors express our thanks to the staff of NIRS-HIMAC for their support during the experiments (p138). This work was carried out as a part of the Research Project with Heavy Ions at NIRS-HIMAC.

Reference

Apel, P. Yu., Akimenko, A. P., Blonskaya, I. V., Cornelius, T., Neumann, Schwarts, K., Spohr, R., Trautmann, C., 2006. Etching of nanopores in polycarbonate irradiated with swift heavy ion at 15K. Nucl. Instrum. Methods B 245, 284-287.

Barillon, R., Fromm, M., Chambaudet, A., Marah, H., Sabir, A., 1997. Track etch velocity study in a radon detector (LR-115, cellulose nitrate). Radiat. Meas. 28, 619-628.

Barillon, R., Fromm, M., Chambaudet, A., Katz, R., Stoquert, J. P., Pape, A., 1999. Bond scission cross sections for α-particles in cellulose nitrate (LR115). Radiat. Meas. 31, 71-75.

Barillon, R., Yamauchi, T., 2003. Chemical bond scission induced by $^{1}H^{+}$, $^{16}O^{8+}$, γ-rays in cellulose nitrate. Nucl. Instrum. Methods B 208, 336-339.

Barillon, R., 2005. Track etch velocity and chemical damages induced by ions in a cellulose nitrate. Radiat. Meas. 40, 214-217.

Bernaola, O. A., Saint Martin. G., Azipiazu Garrido, S. M., 2006. Submicroscopic analysis of damage structure in nuclear. Radiat. Meas. 41, 247-252.

Doerschel, B., Hermsdorf, D., Pieck, S., Starke, S., Thiele, H., Weickert, F., 2003. Studies of SSNTDs made from LR-115 in view of their applicability in radiobiological experiments with alpha partickes. Nucl. Instrum. Methods B 207, 154-164.

Enge, W., 1995. On the question of nuclear track formation in plastic mterial. Radiat. Meas. 25, 11-26.

Fromm, M., 2005. Light MeV-ions etching studies in a plastic track detector. Radiat. Meas. 40, 160-169.

Kovalenko, V. I., Mukhamadeeva, R. M., Maklakova, L. N., Gustova, N. G., 1992. Interpretation of the IR spectrum and structure of cellulose nitrate. Journal of Structural Chemistry 31, 540-547.

Marocco, D., Bochicchio, F., 2001. Experimental determination of LR-115 detector efficiency for exposure to alpha particles. Radiat. Meas. 34, 509-521.

Oganesyan, V. R., Tromimov, V. V., Gaillard, S., Fromm, M., Danziger, M, Hermsdorf, D., Orelovitch O. L., 2005. Investigation of the response of thin CR-39 polymer foils irradiated with light ions. Nucl. Instrum. Methods B 236, 289-294.

Sertova, N., Balanzat, E., Trautmann, C., Toulemonde, M., 2005. Measurements of etching rate of ion tracks: comparison of different approaches. Sixth Int. Sym. Swift Heavy Ions in Matter, May 28-31, 2005, Aschaffenburg, Book of Abstracts B-137.

Yasuda, N., Konishi, Y., Matsumoto, K., Yamauchi, T., Asuka, T., Furusawa, Y., Sato, Y., Oda, K., Tawara, H., Hieda, K., 2005. Dose distribution of carbon ions in air assessed using imaging plates and ionization chamber. Radiat. Meas. 40, 384-388.

Yip, C. W. Y., Nikezic, D., Ho, J. P. Y., Yu, K. N., 2006. Chemical etching characteristics for cellulose nitrate. Materials Chemistry and Physics 95, 307-312.

Zhu, Z. Y., Duan, J. L., Maekawa, Y., Koshikawa, H., Yoshida, M., 2004. Bulk and track etching of PET studied by spectrophotometer. Radiat. Meas. 38, 255-261.

Zhu, Z., Maekawa, Y., Liu, Q., Yoshida, M., 2005. Influence of UV light illumination on latent track structure in PET. Nucl. Instrum. Methods B 236, 61-67.

Figure Captions

Fig. 1 Spectral changes observed in gamma-irradiated LR-115.

Fig. 2 Relative glycosidic bonds and nitrate functions decrease versus gamma-dose.

Fig. 3 Relative glycosidic bonds and nitrate functions decrease versus Fe ion fluences.

Fig. 4 Spectral changes caused by chemical etching in LR-115 exposed to 147 MeV Fe ions.

Fig. 5 Changes in relative C=O bonds in additives during chemical etching.

Fig. 6 Evolution of effective pit radius in LR-115 by chemical etching.

Fig. 7 Track etching velocity of Fe ion track in lR-115.

Table 1

Summary of radio-sensitivity of glycosidic bonds and nitrate function in LR-115.

Bonds			Gamma-ray	Fe ion	
			G-value	G-value	Track Core radius (nm)
Glycosidic bonds	C-O-C	1145 cm^{-1}	58	66	18
Nitrate function	O-NO_2	1600 cm^{-1}	74	76	14

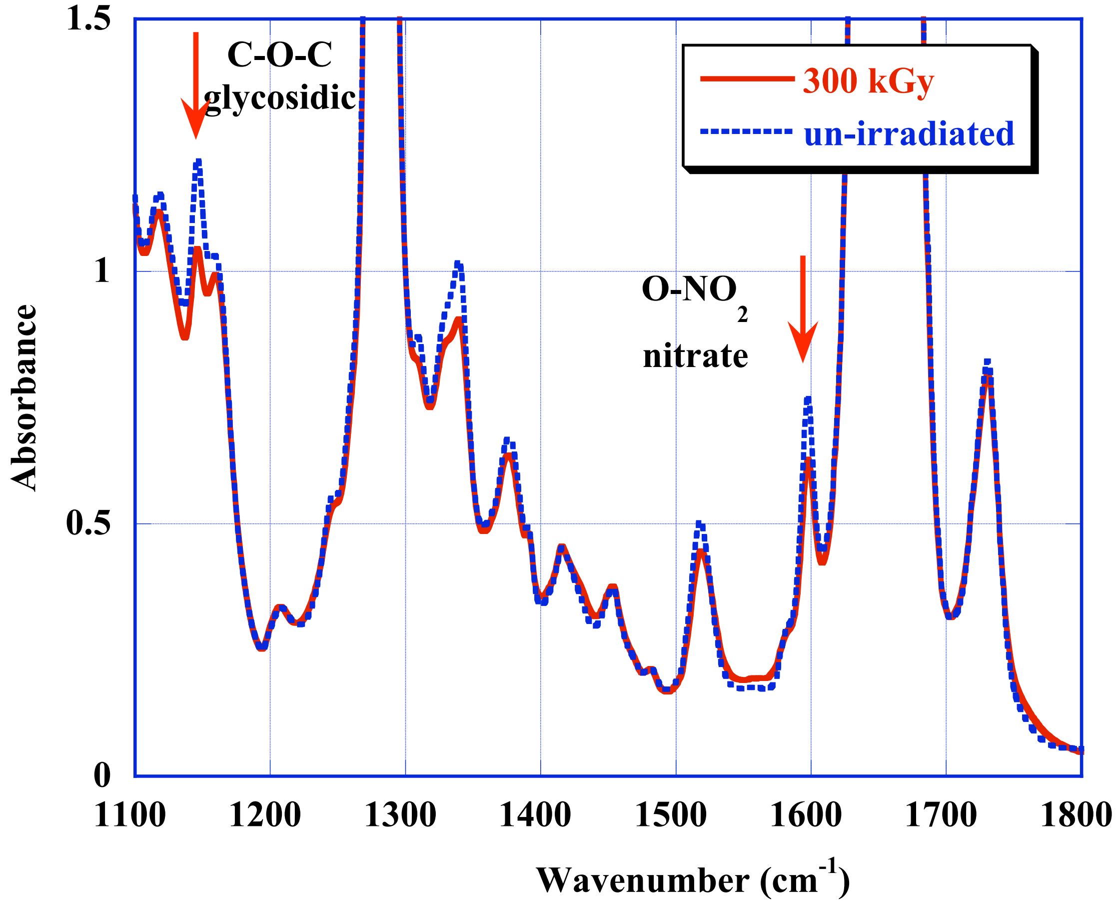
1.5
1
0.5
0
Absorbance
C-O-C
glycosidic
O-NO2
nitrate
300 kGy
un-irradiated
1100
1200
1300
1400
1500
1600
1700
1800
Wavenumber (cm-1)

Fig. 1

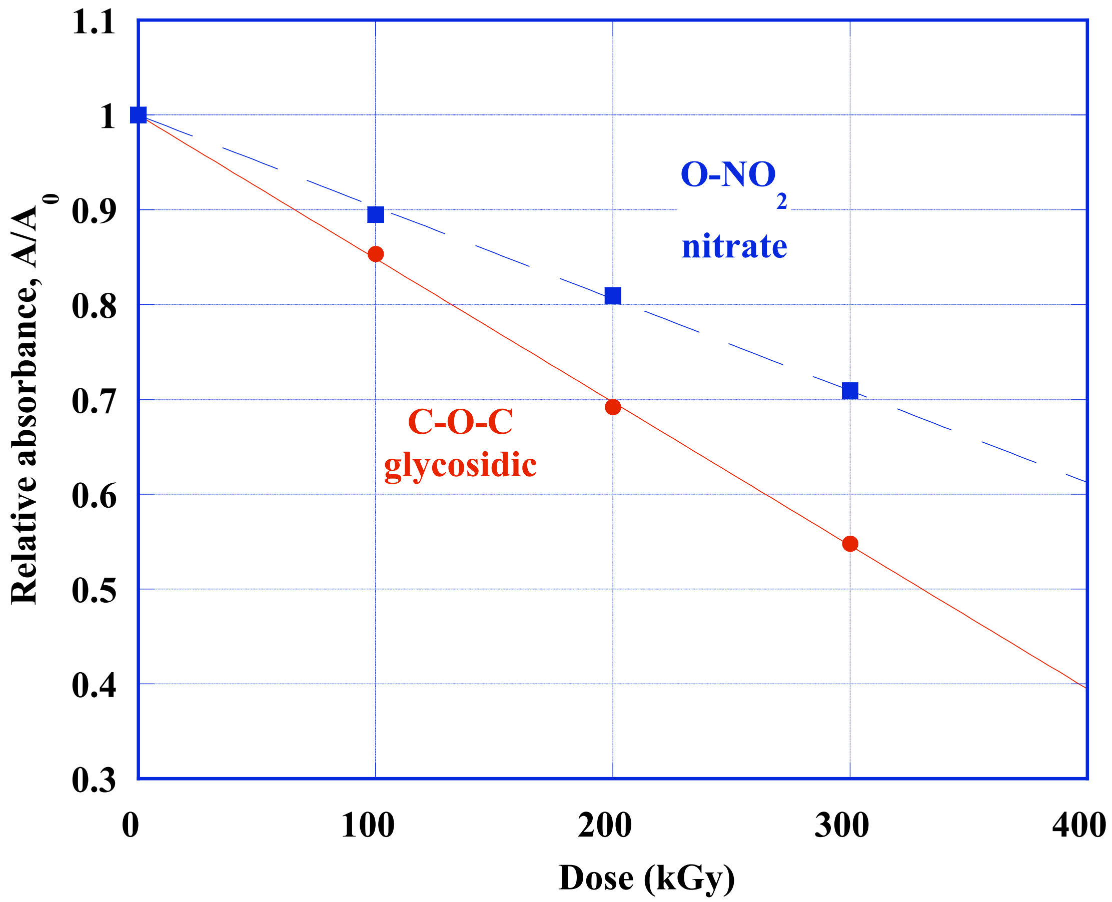
1.1
1
0.9
0.8
0.7
0.6
0.5
0.4
0.3
Relative absorbance, A/A0
0
100
200
300
400
Dose (kGy)
O-NO2
nitrate
C-O-C
glycosidic

Fig. 2

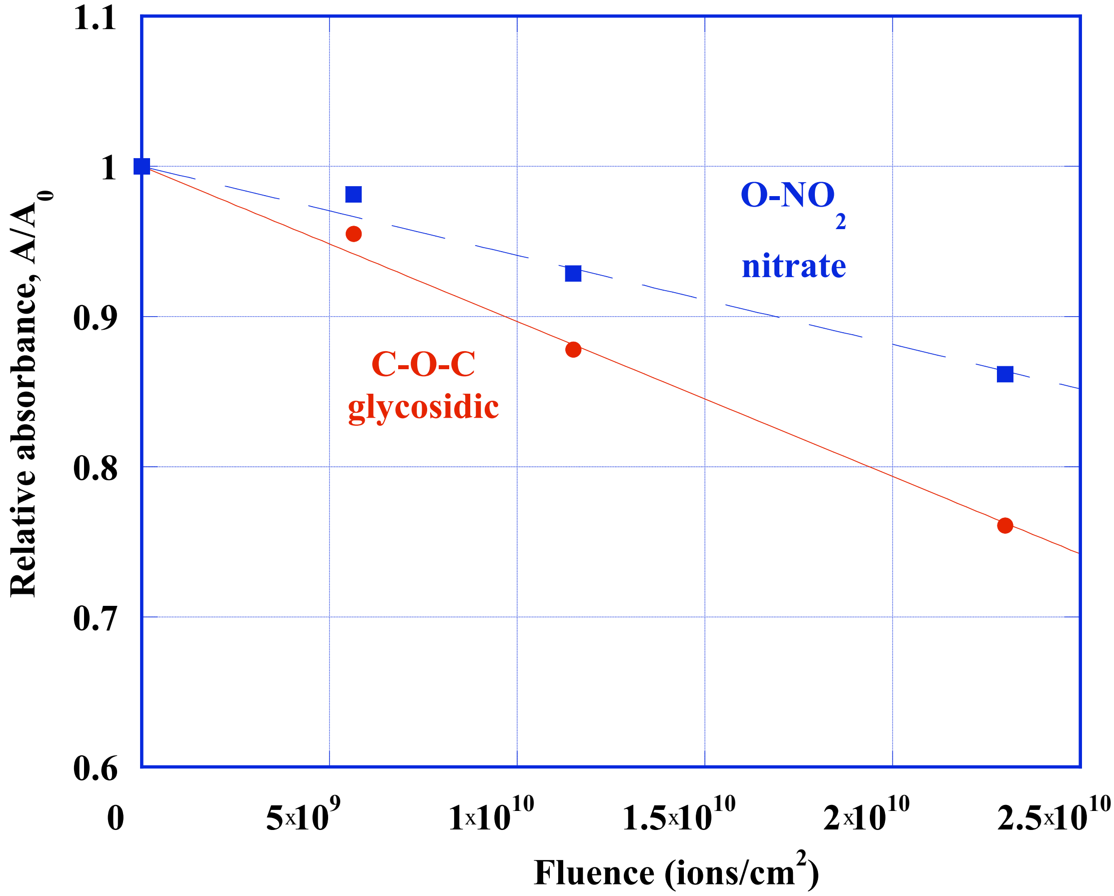
1.1
1
0.9
0.8
0.7
0.6
Relative absorbance, A/A0
0
5x10^9
1x10^10
1.5x10^10
2x10^10
2.5x10^10
Fluence (ions/cm^2)
O-NO2
nitrate
C-O-C
glycosidic

Fig. 3

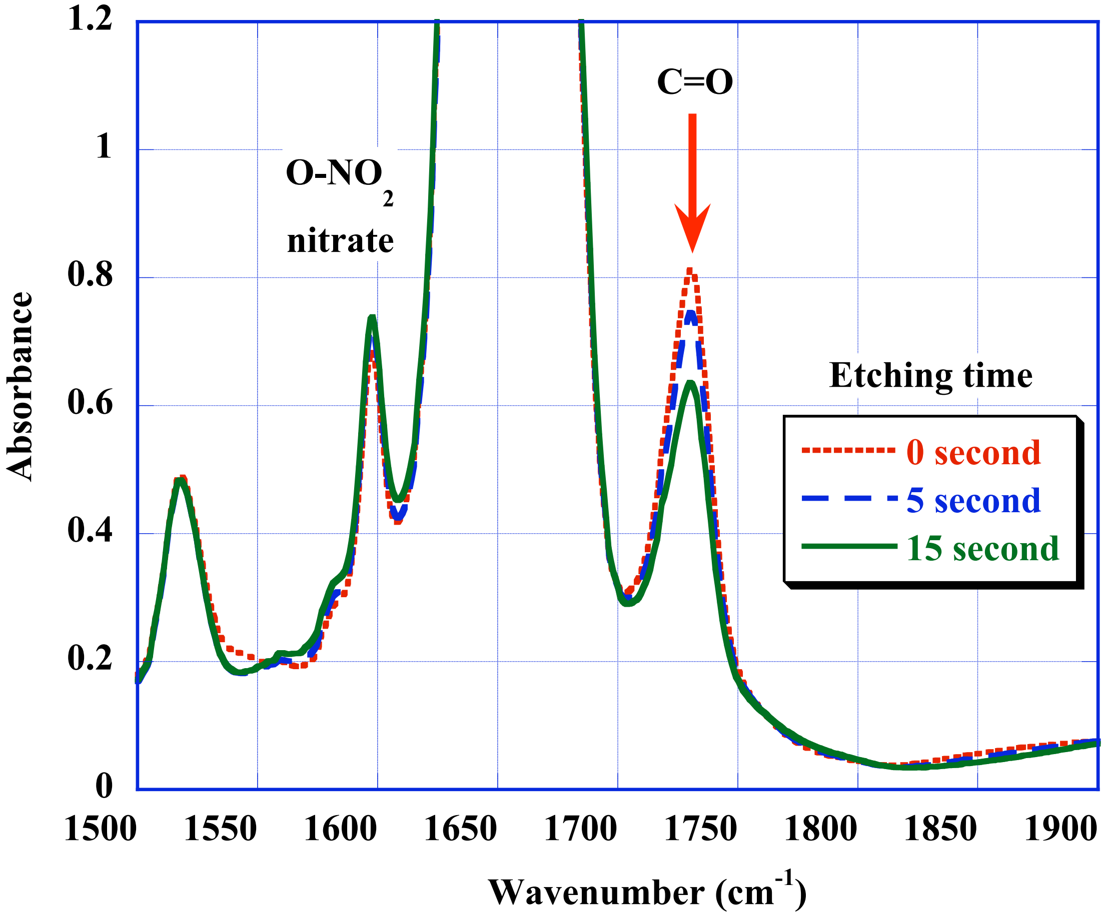

C=O
O-NO2
nitrate
Etching time
0 second
5 second
15 second
Absorbance
Wavenumber (cm-1)
0
0.2
0.4
0.6
0.8
1
1.2
1500
1550
1600
1650
1700
1750
1800
1850
1900

Fig. 4

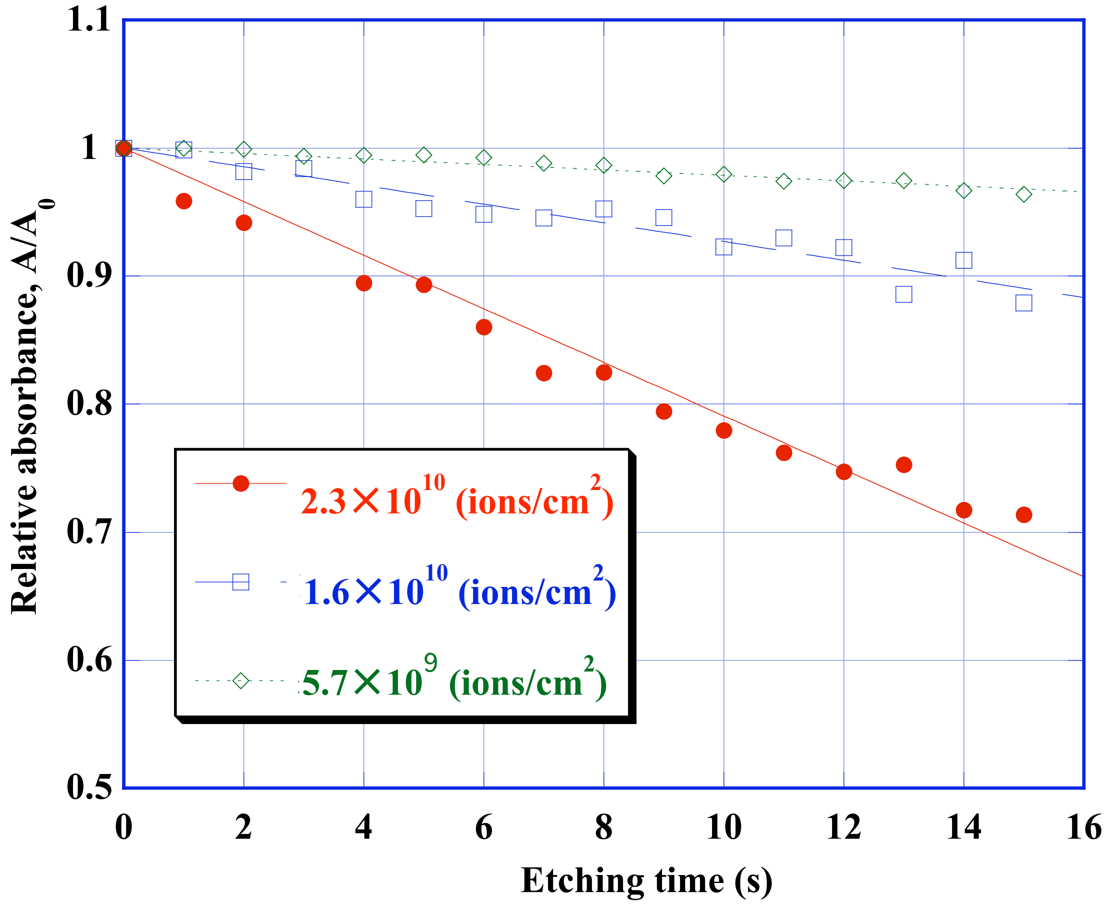

1.1
1
0.9
0.8
0.7
0.6
0.5
0
2
4
6
8
10
12
14
16
Relative absorbance, A/A0
Etching time (s)
2.3×10^10 (ions/cm^2)
1.6×10^10 (ions/cm^2)
5.7×10^9 (ions/cm^2)

Fig. 5

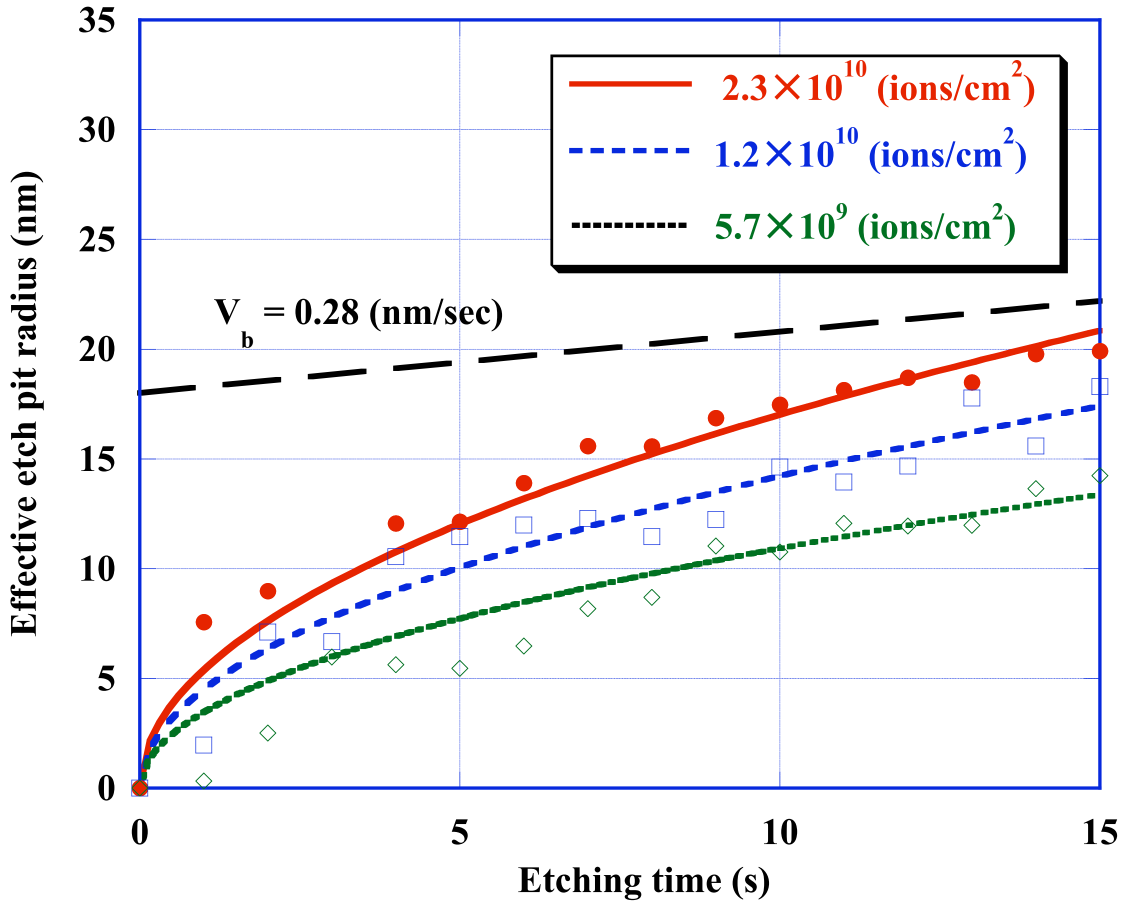

35
30
25
20
15
10
5
0
0
5
10
15
Effective etch pit radius (nm)
Etching time (s)
2.3×10^10 (ions/cm^2)
1.2×10^10 (ions/cm^2)
5.7×10^9 (ions/cm^2)
V b = 0.28 (nm/sec)

Fig. 6

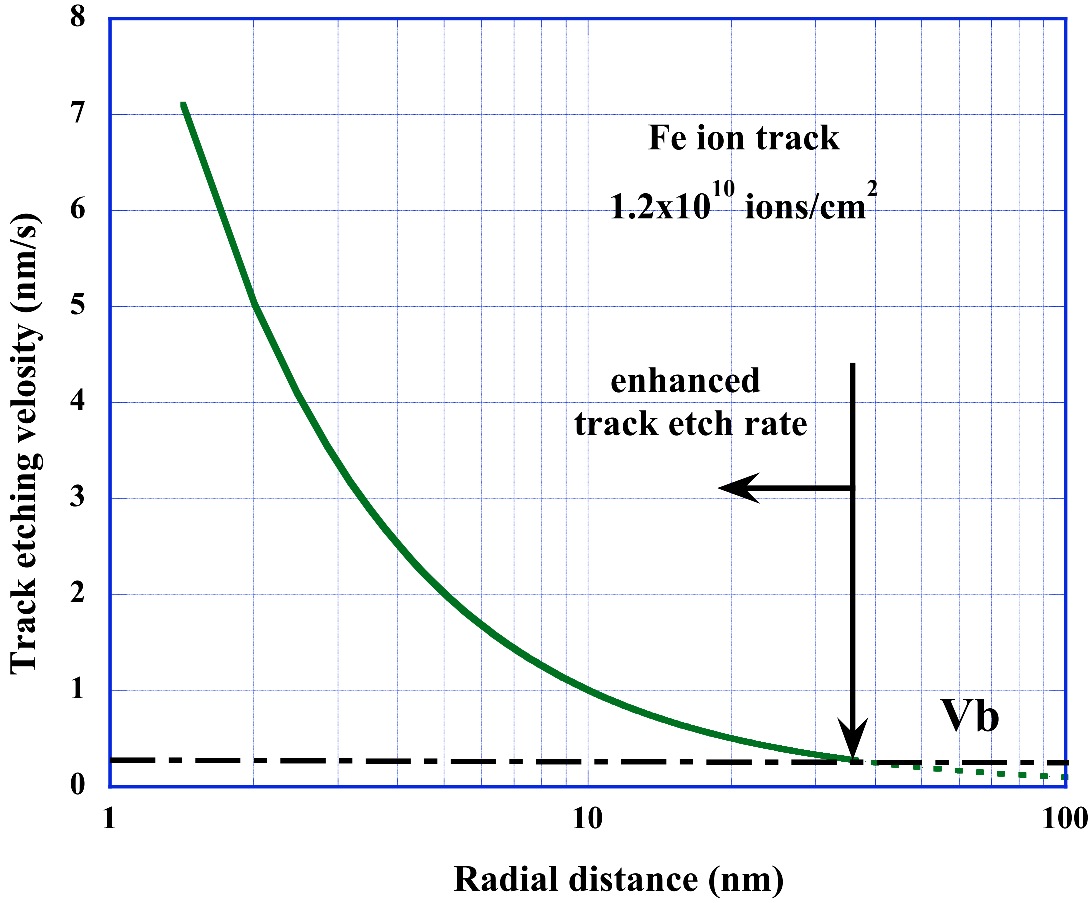
Track etching velocity (nm/s)
8
7
6
5
4
3
2
1
0
1
10
100
Radial distance (nm)
Fe ion track
1.2x10^10 ions/cm^2
enhanced
track etch rate
Vb

Fig. 7